Energy Transfer from a Pulse Network to a Propagating Current Sheet

PAUL J. WILBUR*
Colorado State University, Fort Collins, Colo.

AND

ROBERT G. JAHN†
Princeton University, Princeton, N. J.

The nature of the process of energy transfer from a pulse network to the mass associated with the propagating current sheet in a linear pinch discharge is studied experimentally and analytically. The efficiency of this process is related to the ratios of pulse line impedance/average discharge impedance, and current pulse duration/characteristic acceleration time. Experiments in hydrogen, argon, krypton, and nitrogen at a common ambient mass density and impedance ratios near unity yield efficiencies that exhibit the same qualitative variation with these ratios as those predicted, but only the hydrogen data show good quantitative agreement with the theoretical values. This failure of the theoretical model for the higher molecular weight gases is traced to the existence of diffuse current patterns flowing in the region behind the propagating current sheet, contrary to the theoretical "snowplow" assumption that all of the current flows in a thin sheet.

I. Introduction

REALIZATION of the primary advantage of high specific impulse electric thruster systems—their capacity to deliver large payload fractions over high characteristic velocity missions—is contingent on the efficient conversion of electrical energy into thrust power. If this efficiency is low, the mass of the required powerplant becomes excessive, and detracts from the deliverable payload advantage of this class of propulsion system. The purpose of the work described in this paper is to identify and examine certain factors affecting the efficiency of conversion of electrical energy into thrust energy for a particular type of electric thruster, the pulsed plasma accelerator. Within the scope of this investigation, no attempt has been made to deal with realistic space hardware, or to optimize over-all system performance. Rather, the effort has been confined to matching a particularly simple and well-understood accelerating discharge, the large radius linear pinch,[1] with a pulse power source of conveniently variable characteristics, in this case a lumped element, low-impedance pulse line.[2]

In most conventional power systems, optimum energy transfer efficiency is achieved when the impedance of the load is equal to that of the power source. For example, consider the transfer of energy from an ideal transmission line, initially charged to a voltage V_0, to a resistance connected across its terminals. The transmission line may be characterized by an impedance, $Z_L = (L'/C')^{1/2}$, and a pulse duration, $\tau = 2l(L'C')^{1/2}$, where L' is the inductance per unit length and C' the capacitance per unit length of a line of total length l.[3] For $Z_L > R$, current oscillates back and forth through the load, and several characteristic times are required to achieve substantial energy transfer to the load. For $Z_L < R$, charge is only incompletely removed from the line in the first pulse increment, and several additional wave reflections from the line terminals are needed to complete the energy transfer. Only in the matched case, $Z_L = R$, is all of the energy initially stored in the transmission line transferred to the resistor in one pulse time τ.

If the simple resistive load is replaced by a pulsed plasma accelerator, one might similarly expect optimum energy transfer when the discharge impedance is equal to the driving line impedance, provided also that the pulse duration is properly matched to some characteristic acceleration time. However, the impedance implicit in the dynamical development of a gas accelerating discharge is not adequately represented by an equivalent resistance, and this complication reflects itself into substantial distortion of the simple impedance match criterion.

II. Theoretical Analysis

A pulsed plasma accelerator functions by establishing a narrow, intense current sheet which is driven by its self-magnetic field to accumulate ambient gas it overruns. The dynamics of the current sheet motion can be most simply described by a "snowplow" relation[4] which expresses a balance between the $\mathbf{j} \times \mathbf{B}$ body force and the time rate of change of momentum associated with the accumulation and acceleration of mass on the current sheet. For example, the equation in linear pinch geometry (Fig. 1) takes the form

$$r(d/dt)[(r_1^2 - r^2)dr/dt] = -\mu_0 I^2/4\pi^2\rho \qquad (1)$$

where μ_0 is the permeability of free space, I is the total current flowing through the discharge chamber, and ρ is the ambient gas density in the discharge chamber of radius r_1. The radius of the cylindrical current sheet, r, through which I is assumed to flow, also defines an inductance of the discharge through the relation[3]

$$L_D = (\mu_0 h/2\pi) \ln(r_0/r) \qquad (2)$$

The voltage drop across the discharge is given by

$$V_{CH} = IR_D + d\phi/dt = IR_D + (d/dt)(IL_D) \qquad (3)$$

where R_D is the resistance of the discharge, ϕ is the magnetic flux linked by the discharge, and L_D is the inductance defined by Eq. (2).

Presented as Paper 69-113 at the AIAA 7th Aerospace Sciences Meeting, New York, January 20–22, 1969; submitted January 31, 1969; revision received June 5, 1969. This program is supported by NASA Grant NGL 31-001-005.

* Assistant Professor, Mechanical Engineering Department. Member AIAA.

† Professor of Aerospace Sciences, Guggenheim Aerospace Propulsion Laboratories. Associate Fellow AIAA.

In these experiments, as in most operative thrusters, the circuit also contains a switch, which to a good approximation may be represented as a fixed resistance and inductance, R_s and L_s. The switch and discharge chamber comprise the total load driven by the pulse line, and the voltage across this load may therefore be written

$$V_T = (R_D + R_s)I + L_s dI/dt + (d/dt)(L_D I) \qquad (4)$$

The pulse line power source may be described by Kirchoff's equations applied to each loop and node in the pulse network (Fig. 2)

$$\left.\begin{aligned} dQ_1/dt &= I_1 - I \\ &\cdot \\ &\cdot \\ &\cdot \\ dQ_i/dt &= I_i - I_{i-1} \\ &\cdot \\ &\cdot \\ &\cdot \\ dQ_n/dt &= -I_{n-1} \end{aligned}\right\} \ (n \text{ equations}) \qquad (5)$$

and

$$\left.\begin{aligned} dI/dt &= (V_T - Q_1/C)/L \\ &\cdot \\ &\cdot \\ &\cdot \\ dI_i/dt &= (Q_{i+1} - Q_i)/LC \\ &\cdot \\ &\cdot \\ &\cdot \\ dI_{n-1}/dt &= (Q_n - Q_{n-1})/LC \end{aligned}\right\} \ (n \text{ equations}) \qquad (6)$$

where Q_i represents the electrical charge on the ith capacitor. This n station LC ladder network may also be described by a nominal line impedance and a pulse duration corresponding to those given for the ideal transmission line,[5] i.e., $Z_L = (L/C)^{1/2}$ and $\tau = 2n(LC)^{1/2}$.

Equations (1, 2, 4, 5, and 6) are $2n + 3$ equations in $2n + 3$ dependent variables (n pulse line currents, n pulse line capacitor charges, V_T, r, and L_D) and the independent variable time which describe the behavior of the pinch discharge pulse line system. They have been solved here on the digital computer using a Runge-Kutta technique. Figure 3 shows current and voltage waveforms and the current sheet trajectory computed for a set of input parameters typical of those prevailing in the experiments. Figure 3a shows the total current flowing through the switch and pinch chamber as a function of time, compared with that for an ideal pulse line discharged through a matched resistance. The time τ_{ej} shown on all of the ordinates of Fig. 3 is the characteristic time over which the acceleration of the current sheet occurs. In an actual thruster τ_{ej} would be the time of ejection of the plasma, determined by the length of the thruster, but for the closed chamber geometry considered here the plasma is considered "ejected" when the sheet reaches a 1-in. radius. One inch was selected because accurate experimental investigation is difficult at lesser radii and yet the acceleration process should be allowed to occur over as large a distance as possible in order to prevent the initiation effects from dominating the behavior of the system. Figure 3b shows the voltage across the end of the pulse line (i.e., across the switch and discharge chamber) as a function of time compared with the corresponding matched impedance voltage waveform for a purely resistive load.

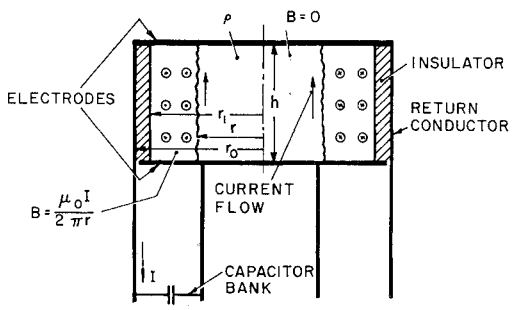

Fig. 1 Pinch discharge configuration.

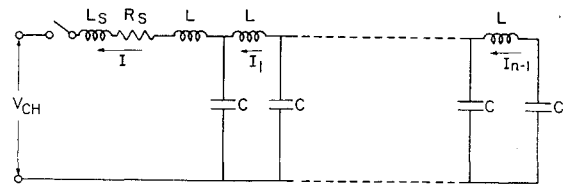

Fig. 2 Schematic of pulse line-accelerator system.

The evident distortions of the current and voltage waveforms from the idealized case can be assigned to the following causes.

1) The initial inductance associated with the switch and discharge configuration constrains the current to a finite rise time.

2) Unlike the constant resistive load, the "impedance" of the discharge varies with time, has both resistive and reactive components, and is a function of both the discharge and the power source characteristics. The concept of an impedance, as such, is thus somewhat artificial in this situation, but may still be used to denote the instantaneous ratio of the voltage across the discharge chamber [Eq. (3)] to the discharge current:

$$Z_D = V_{CH}/I = R_D + dL_D/dt + (L_D/I)dI/dt \qquad (7)$$

Since the plasma resistance is small and the current pulses are nearly flattopped, the second term dominates this expression, yielding, from Eq. (2),

$$Z_D \approx dL_D/dt = (\mu_0 h/2\pi r)dr/dt \qquad (8)$$

The current sheet trajectory of Fig. 3c shows an increasing velocity with decreasing radius, both of which contribute

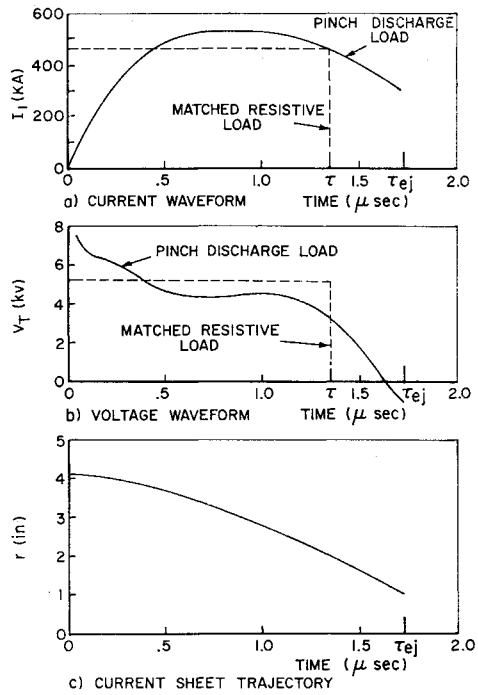

Fig. 3 Theoretical results: $R_s = 0.002\ \Omega$, $R_D = 0.0001\ \Omega$, $r_0 = 0.117$ m, $r_1 = 0.105$ m, $h = 0.0508$ m, $L_s = 3.00 \times 10^{-9}$ h, $\rho = 0.00022$ kg/m^3, $\tau = 2\ n(LC)^{1/2} = 1.3 \times 10^{-6}$ sec, $Z_L = (L/C)^{1/2} = 0.00113\ \Omega$, $V_0 = 10{,}500$ v.

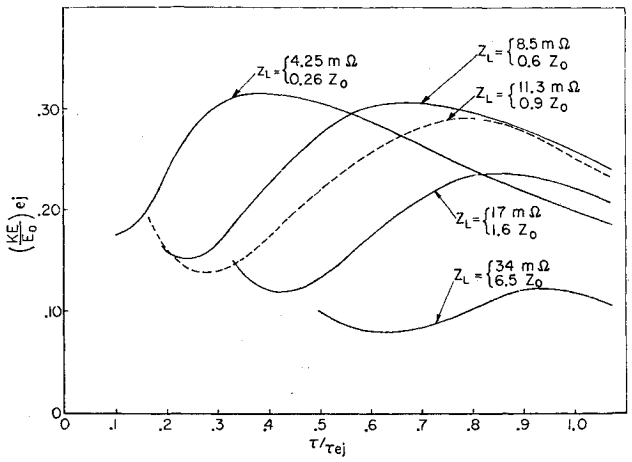

Fig. 4 Effect of pulse length and impedance on efficiency.

to an impedance that increases with time. This effect causes the voltage to rise and current to drop once the initial rise time has elapsed.

3) Since the inductance of the discharge, which is small initially, increases to a relatively large value as the discharge proceeds, a considerable amount of energy is stored in the magnetic field of the discharge at the time the pulse begins to decay. This causes the current to continue to flow after the voltage across the discharge chamber reverses. If the characteristic ejection time, τ_{ej}, is long compared to the pulse length, τ, the energy stored in this field will be transferred, in part at least, back into the pulse network and will later produce a negative current through the discharge chamber. Even under conditions where the average impedance of the discharge is much greater than that of the line, the negative current is predicted. In such cases the current pulse is protracted far beyond the pulse duration time, τ, somewhat similar to the stepwise decay of an overdamped resistive load, but the large inductive effects eventually force sufficient negative voltage onto the pulse line to cause the current reversal.

The analysis used to obtain the current and voltage also yields the distribution of energy in the pulse network, switch, and discharge chamber. This energy may appear in the following forms:

1) Energy stored capacitively in the electric fields and inductively in the magnetic fields of the pulse network.

2) Energy stored inductively in the magnetic field associated with the switch discharge.

3) Energy stored inductively in the magnetic field of the main discharge.

4) Kinetic energy of the mass accumulated on the propagating current sheet. In the spirit of this study, it is this organized streaming motion of the propellant mass which represents the thrust energy of the accelerator, and is the component to be optimized.

5) Energy invested in ionization, dissociation, excitation, and random thermal modes of the plasma. Energy input of this category can enter the theoretical model via the following two mechanisms: a) the resistive heating input due to the plasma resistance R_D, and b) the gasdynamic loss associated with acceleration of particles initially at rest to the current sheet velocity as a result of collisions with particles already collected. This loss, which is required to satisfy energy conservation under the constraint of momentum conservation as expressed by the snowplow equation, is discussed in Ref. 6.

6) Thermal energy deposition in the switch plasma.

Although it is quite possible that thermal energy in the accelerated plasma may be converted into thrust energy, the efficiency of the pulsed plasma accelerator is defined conservatively here as the ratio of the organized kinetic energy measured at the characteristic ejection time, KE_{ej}, to the initial energy stored in the pulse line, E_0. The efficiency so defined is found to be a function of both the relative impedance match between the line and the load, and of the relative magnitudes of the pulse duration τ and the ejection time τ_{ej}. For example, variation of the pulse duration by changing the number of stations in the pulse line while holding the line impedance constant ($Z_L = 11.3\ m\Omega$) results in the efficiency curve shown in Fig. 4 as a dotted line. The quantity Z_0 shown as a parameter is an average discharge impedance calculated using Eq. (8) and the sheet velocity at midradius. The time average of the impedance is approximately equal to the impedance at this radius, except for very short pulse durations, $\tau/\tau_{ej} < 0.5$, which are outside the range of primary interest.

For current pulse lengths substantially less than the pulse length producing peak efficiency at this impedance, the magnitude of the current is less than the maximum value over a large fraction of the acceleration time and hence the current sheet accelerates less vigorously and a proportionately smaller fraction of the initial line energy is transferred into kinetic energy of the sheet. As the pulse length is increased the current remains high for a larger fraction of the acceleration time and the current sheet acquires a larger fraction of the initial energy. Increases in pulse length beyond the optimum value result in a decrease in efficiency because a considerable fraction of the initial line energy remains in the pulse line and in magnetic fields associated with the switch and the discharge at τ_{ej}.

For very short pulse lengths, the current waveform may go through two or more half cycles before τ_{ej}, and the efficiency will go through corresponding local maxima and minima. This analysis is not extended to the very short pulses producing these subsequent maxima because the theoretical model used here is known to break down when current reversal occurs because of the generation of secondary current sheets.

If one allows both the pulse length and the characteristic impedance of the pulse line to vary, the complete series of curves shown in Fig. 4 is obtained. These curves show that the pulse duration corresponding to the peak efficiency decreases with the characteristic line impedance. Of primary interest, however, is the locus of the maxima of the set of curves, shown in Fig. 5 as a function of the driving line impedance. Also plotted for comparison is the efficiency of energy transfer from a transmission line to a pure resistance within a time equal to the pulse duration of the line.

Note that whereas the maximum efficiency for the resistive load is achieved when the impedance of the line is equal to the resistance of the load, the efficiency of transfer to the pinch discharge load shows no such maximum as a function of driving line impedance. Rather there is a monotonic increase of efficiency with reduction of Z_L. This effect is

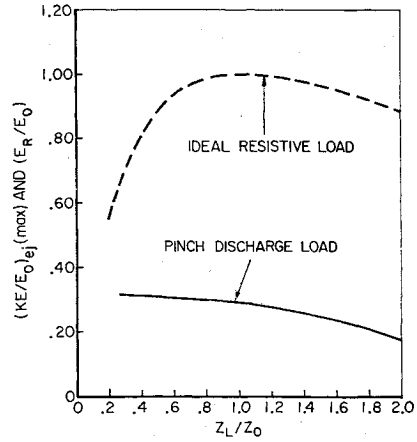

Fig. 5 Efficiencies vs pulse line impedance.

attributable to the more vigorously accelerating current sheets produced by the lower impedance, higher current sources. Rapidly accelerating sheets are known to sustain less energy loss to thermal modes as a result of gasdynamic effects,[6] and this gain more than balances the electrical inefficiency associated with the increasing impedance mismatch. The large difference in magnitude of the two curves of Fig. 5 is due primarily to the method of defining efficiency for the accelerator, and may be somewhat misleading. Much of the energy not transferred to directed kinetic motion of the plasma has been deposited in it in thermal form so that, in this sense, a major portion of the initial line energy has been delivered to the "load." In addition, no effort has been made here to optimize the efficiency through selection of the discharge and switch characteristics; rather the calculations presented are those corresponding to the experimental conditions encountered in the laboratory equipment. In this equipment the losses in the switch are quite large, and they account for a significant reduction in the magnitude of the efficiency.

III. Experimental Behavior

In order to verify the mathematical description and characteristic properties of the pulse line without the complication of the pinch discharge, typical pulse line configurations were discharged through a resistor capable of withstanding the high currents and voltages produced when such a line is discharged from 10 kv. The mathematical model described in the preceding section was modified by substituting a resistance and fixed inductance for the equations describing the dynamics of the discharge. The extent of the agreement between the mathematical model and the actual pulse line is shown in Fig. 6. The waveforms differ from the ideal squarewaves observed when a transmission line is discharged through a resistor, first because this line has lumped elements, rather than distributed parameters, and second because the included inductance associated with the resistor and switch restrain the rate of rise and decay of the current at the beginning and end of the pulse.

The measured capacitance and inductance of the average unit used in these experiments are 6.35 ± 0.05 μf and 7.5 ± 0.4 nh.‡ They are designed to permit low-inductance connection of adjacent units thereby facilitating variation

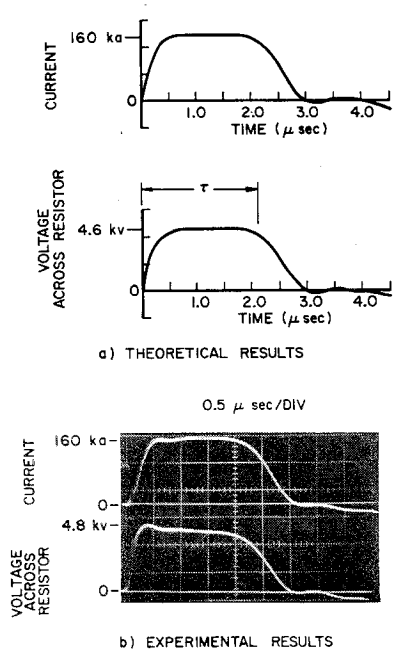

Fig. 6 Theoretical and experimental waveforms from matched pulse line.

‡ These prototype low-inductance capacitors were developed in conjunction with the Corson Manufacturing Corp.

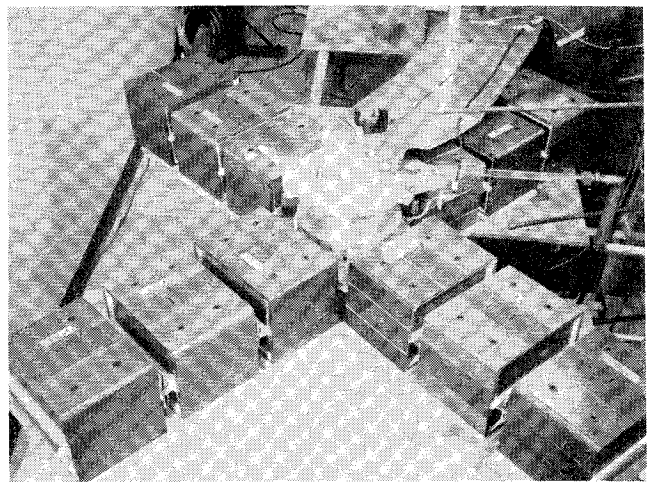

Fig. 7 Typical capacitor configuration.

of the pulse duration and the characteristic line impedance. Pulse duration is varied by changing the number of stations in a line of capacitors (i.e., the number of units connected in tandem). Line impedance is varied by changing the number of these lines connected in parallel across the discharge chamber. Figure 7 shows a typical configuration with 12 of the units arranged around the discharge chamber to produce a pulse three times the length (three units in tandem) and one-fourth the impedance (four lines of units in parallel) of the single unit pulse.

Experimental evaluation of the efficiency (KE_{ej}/E_0) requires the determination of organized kinetic motion of the current sheet mass, in ratio to the initial line energy, which is one-half the product of charging voltage squared and total capacitance. Since direct measurement of the energy in organized kinetic motion of the current sheet is not feasible in a closed discharge chamber, this determination is based on the assumption that all of the mass the current sheet encounters is collected and accelerated, i.e., that the snowplow model is a valid representation of the physical process. This reduces the problem to measurement of the velocity of the mass associated with the current sheet. York,[7] who has developed a new fast response pressure probe, has found that the arrival of the current sheet, sensed by a magnetic field probe, precedes very slightly the arrival of the associated mass motion, sensed by the pressure probe, but that this separation remains essentially constant over most of the trajectory. In view of this correlation, the physically smaller and simpler magnetic field probes were used to determine current sheet velocities and these are assumed to be the same as those of the mass trajectories. Probes were located along a common radius because errors in the measurement of current sheet velocity associated with probing in the wake of another probe were found to be far less than those due to azimuthal current sheet irregularities over sufficient angular separation to keep probes out of each other's wake.

The experimental measurements discussed previously have been made in argon at an ambient density of 2.2×10^{-4} kg/m^3 and $V_0 = 10.5$ kv for various pulse durations and pulse line impedances, and efficiencies based on these measurements are presented in Fig. 9. The corresponding theoretical curves are shown in Fig. 8. The points on the theoretical curves correspond to data points similarly located on the experimental curves.

Although the snowplow model used in the theoretical calculations requires only the gas density as an input, it may be that other gas properties such as ionization potential, molecular weight, or conductivity play an important role in the acceleration process under the efficient energy transfer conditions at which these experiments were performed. In order to investigate possible effects due to gas properties,

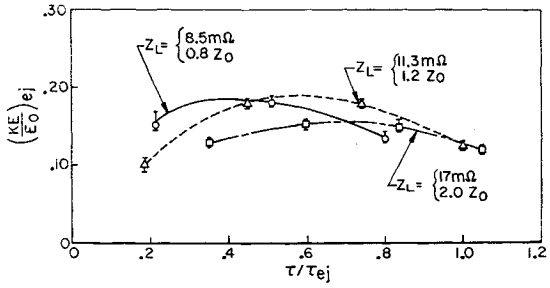

Fig. 8 Efficiency profiles: theoretical.

measurements were also made in nitrogen, krypton, and hydrogen. These measurements were made at the same ambient mass density as those in argon, and therefore the efficiency curves presented in Figs. 10, 11, and 12 should also correspond to the theoretical curves of Fig. 8.

The following qualitative agreements between the experimental and theoretical results can be identified: 1) for a line of a given impedance there is one length of line which gives an optimum efficiency, and 2) as the impedance of the pulse line is decreased the corresponding optimum pulse length for the line also decreases.

The following differences between the theoretical and experimental results obtained in argon, nitrogen, and krypton are, however, also apparent: 1) rather than showing the theoretically predicted increasing optimum efficiency with decreasing pulse line impedance, the experimental curves show a leveling of this locus of the efficiency maxima near an impedance ratio of one; 2) the optimum pulse lengths for lines of given impedance are lower than the corresponding theoretical values; 3) because the experimental velocities are somewhat lower than the calculated values, impedance ratios Z_L/Z_0 specified on the experimental curves are higher than those on the corresponding theoretical curves; 4) the magnitudes of the measured efficiencies are significantly less than those predicted theoretically.

The hydrogen data of Fig. 12, unlike those of the other gases, show good agreement in both magnitude and qualitative behavior with the theoretical results. The improved correlation reflects the fact that current sheet velocities measured in hydrogen correspond much more closely to the theoretical velocities than the velocities measured in the heavier test gases. The greater experimental scatter in the hydrogen data occurs because dB/dt peaks used to determine current sheet velocities are not as reproducible or as well defined in hydrogen as they are in the other test gases.

The discrepancies between theoretically predicted and measured velocities in the heavier gases which result in the lower experimental efficiencies can be assigned to a failure of all of the current flowing through the discharge chamber to concentrate in a thin sheet as the snowplow model assumes. Any current which flows in the region behind the advancing current sheet reduces the inductance [Eq. (2)] and the impedance [Eq. (8)] of the discharge, thereby predicating a lower velocity sheet. Evidence that the current flowing in

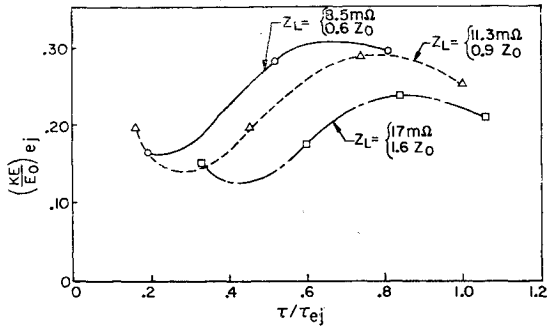

Fig. 9 Efficiency profiles: argon (experimental).

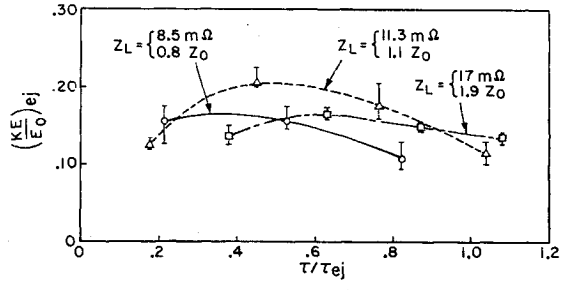

Fig. 10 Efficiency profiles: nitrogen (experimental).

the discharge chamber is not confined to a thin sheet can be presented in the form of discharge chamber current and voltage oscillograms obtained in hydrogen and argon, compared with the corresponding theoretically predicted waveforms (Fig. 13). The theoretical curves of Fig. 13a display the increase of discharge impedance with current sheet progress which forces the current magnitude to decrease and the discharge chamber voltage to rise after the initial characteristic current rise time. The experimental waveforms obtained in hydrogen (Fig. 13b) exhibit this same type of behavior, but the corresponding waveforms obtained in argon (Fig. 13c) show the discharge chamber voltage decaying and the current continuing to rise at a lesser rate, long after the characteristic rise time. Such behavior can exist only if the net discharge impedance is decreasing. Since measured trajectories show the current sheet is *accelerating* inward during this period (increasing impedance), parallel current paths must exist which cause the decrease in net impedance observed in the argon waveforms.

This effect may be illustrated more directly by rewriting Eqs. (2) and (3) in the form

$$L_D(t) = \left(\int_0^t [V_{CH}(\xi) - I(\xi)R_D]d\xi \Big/ I(t)\right) \tag{9}$$

$$r(t) = r_0 \exp - [2\pi L_D(t)/\mu_0 h] \tag{10}$$

and applying them to the voltage and current data of Fig. 13, together with the measured resistance of the discharge ($R_D = 10^{-4}$ ohms), to obtain first the net inductance seen by the pulse line and then the trajectory of the mean current flowing in the discharge chamber which corresponds to this net inductance. These trajectories, which are shown in Figs. 14b and 14c for hydrogen and argon are labeled "mean current." The trajectory of the high-current density sheet, on the other hand, is determined experimentally by sensing the time of arrival of the peak of current density with a magnetic probe and is shown in Figs. 14b and 14c as "dB/dt trajectory." For the ideal snowplow model the mean current and peak current density trajectories are clearly identical (Fig. 14a) and for the hydrogen data they show a close correspondence, but for the typical argon discharge the mean current trajectory lags behind the trajectory of the maximum current density. This implies that the experimental inductance and time derivative of inductance are less than the ideal snowplow model predicts and thus that the discrepancy between the theoretical and experimental efficiency is due

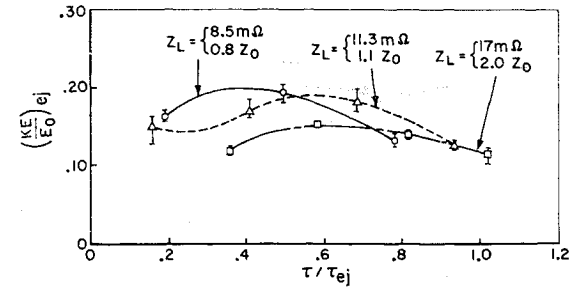

Fig. 11 Efficiency profiles: krypton (experimental).

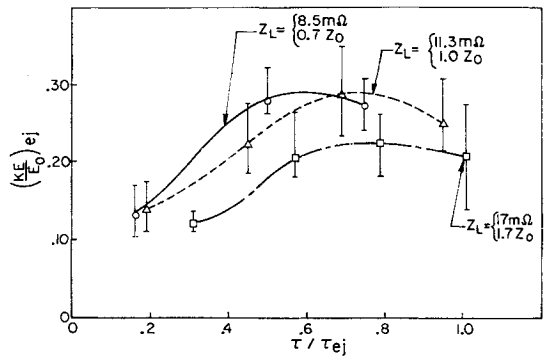

Fig. 12 Efficiency profiles: hydrogen (experimental).

to the failure of the model to account for the diffuse current pattern set up in the discharge chamber behind the propagating high-current density sheet. Additional evidence for the existence of a diffuse current pattern can be found in the magnetic probe records, but quantitative interpretation of these records is difficult because the probes produce local perturbations in the magnitude of the magnetic field under near impedance match conditions.

IV. Summary

The efficiency of energy transfer from a current pulse network into organized motion of the mass associated with the propagating current sheet of a pulsed plasma accelerator has been studied theoretically and experimentally. The theory, which is based on a "snowplow" model, predicts maximum efficiency when the current sheet is driven by a pulse line that 1) has an impedance significantly below the average discharge impedance and 2) produces a pulse that exhibits current reversal near the time when the mass would be expelled from the accelerator. The experimental results suggest the optimum efficiency will be realized when the line impedance is near the discharge impedance, but otherwise confirm the predicted qualitative variation of efficiency with pulse line impedance and pulse duration. The magnitudes of efficiencies in argon, krypton, and nitrogen are observed to be considerably less than the theoretical values, and these quantitative discrepancies have been related to the failure of the snowplow model to account for a fraction of the current which does not flow through the propagating high-current density sheet. Hydrogen data that correlate more closely with the theoretical results manifest a larger fraction of the current flow through the sheet.

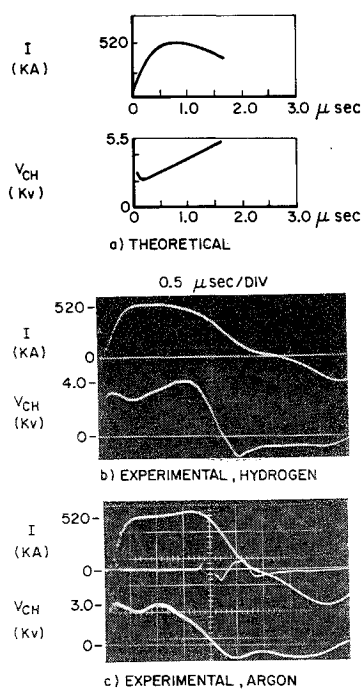

Fig. 13 Voltage and current waveforms: $\rho = 0.00022 kg/m^3$, $V_0 = 10{,}500$ v, $\tau = 1.7$ μsec, $Z_L = 0.0113$ Ω.

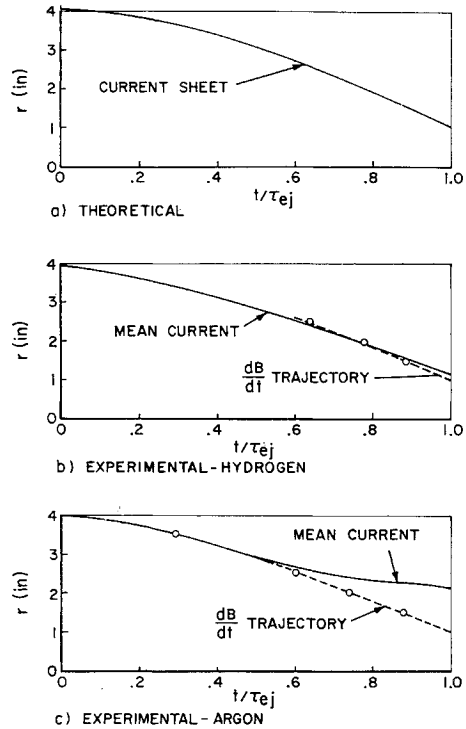

Fig. 14 Current trajectories: $\rho = 0.00022$ kg/m³, $V_0 = 10{,}500$ v, $\tau = 1.7$ μsec, $Z_L = 0.0113$ Ω.

References

[1] Jahn, R. G. and von Jaskowsky, W., "Current Distributions in Large-radius Pinch Discharges," *AIAA Journal*, Vol. 2, No. 10, Oct. 1964, pp. 1794–1753.

[2] Black, N. A. and Jahn, R. G., "Dynamics of a Pinch Discharge Driven by a High-current Pulse-forming Network," Aerospace and Mechanical Sciences Rept. 778, May 1966, Princeton Univ., Princeton, N. J.

[3] Ramo, S., Whinnery, J. R., and Van Duzer, T., *Fields and Waves in Communication Electronics*, Wiley, New York, 1965.

[4] Garwin, R. L. and Rosenbluth, M., "An Infinite Conductivity Theory of the Pinch," TR LA-1850, 1954, Los Alamos Scientific Lab., Los Alamos, N. Mex.

[5] White, H. J., Gillette, P. R., and Lebacqz, J. V., "The Pulse-forming Network," Vol. 5, *Pulse Generators*, edited by G. N. Glasoe and J. V. Lebacqz, M.I.T. Radiation Lab. Series, McGraw-Hill, New York, 1968, Chap. 6.

[6] Black, N. A. and Jahn, R. G., "Dynamic Efficiency of Pulsed Plasma Accelerators," *AIAA Journal*, Vol. 3, No. 6, June 1965, pp. 1209–1210.

[7] York, T. M., "Pressure Distribution in the Structure of a Propagating Current Sheet," Ph.D. thesis, Dec. 1968, Princeton Univ., Princeton, N. J.